

Photoscattering effect in supercontinuum-generating photonic crystal fiber

H. Tu,^{a)} D. L. Marks, Z. Jiang, and S. A. Bopp^{b)}

*Biophotonics Imaging Laboratory, Beckman Institute for Advanced Science and Technology,
University of Illinois at Urbana-Champaign, Urbana, Illinois 61801, USA*

(Received 16 December 2007; accepted 22 January 2008; published online 12 February 2008)

A photosensitivity different from that responsible for fiber grating inscription is found in a supercontinuum-generating photonic crystal fiber transmitting intense 818 nm femtosecond pulses. This photosensitivity progressively generates a waveguide at the entrance of the fiber to scatter light of specific wavelengths and is termed as the photoscattering effect. This effect is linked to the ~ 800 nm photosensitivity in the microlithography of bulk silica glass. While the effect somewhat limits fiber-optic supercontinuum applications, it can be beneficial to produce new photonic devices. © 2008 American Institute of Physics. [DOI: 10.1063/1.2857495]

In a previous study,¹ we reported a relatively surprising photosensitivity for supercontinuum (SC) generating heavily Ge-doped germanosilicate fibers. That is, the prolonged exposure of ~ 800 nm femtosecond pulses produces a multi-millimeter long waveguide at the fiber entrance to dramatically decrease the fiber transmission property over a broad spectral range. This phenomenon resembles the photodarkening effect widely observed in rare-earth doped silica fibers if the Ge dopant plays the role of the rare-earth ions to produce certain absorptive photoproducts.² Alternatively, it resembles the type I photosensitivity well documented in germanosilicate fiber grating inscription in terms that the waveguide is thermally erasable.³ The observed reduction of fiber transmission may be due to the formation of a structure analogous to a long period grating (LPG), which can attenuate fiber transmission by coupling light from core modes into cladding modes. The nature of the photosensitivity remains controversial mainly because the role of the Ge dopant is unclear. In this work, we report the presence of this photosensitivity in a pure silica photonic crystal fiber (PCF) so that no special photosensitive impurity is essential for such photosensitivity. We study the mechanism underlying the near-infrared photosensitivity, which has not been reported in PCFs, and point out its potential applications.

The PCF (LMA-8, Crystal Fibre A/S) under study is an endlessly single-mode pure silica fiber having a cross section of hexagonally arranged $1.7 \mu\text{m}$ diameter air holes with a pitch size of $4.9 \mu\text{m}$. The absence of the central hole results in a core diameter of $8.5 \mu\text{m}$, a mode field diameter of $6.0 \mu\text{m}$, and a numerical aperture (NA) of 0.10 (at 818 nm). The zero dispersion wavelength of the fiber is estimated to be $1.1 \mu\text{m}$.⁴ The pump laser is a 250 kHz regenerative amplifier (Reg9000, Coherent) pulsed at 818 nm with ~ 25 nm full width at half maximum bandwidth. The 1 mm diameter laser beam is coupled into the fiber by a NA of 0.40, 5.0 mm diameter aspheric lens. The pulse energy (pump power) is varied by a neutral-density filter between 0.04 and $1 \mu\text{J}$ (10–250 mW). The pulse width is controlled by a compressor to yield transform-limited 35 fs or positively chirped 210 fs pulses immediately before the aspheric lens, as measured by an autocorrelator. The initial ~ 10 mm of the fiber (~ 0.5 m total length) is stripped of acrylate coating. The

initial ~ 100 mm of the fiber is mounted straight on a three-axis fiber positioner, which maximizes the fiber coupling efficiency. The SC spectrum is monitored by a spectrometer (USB2000, Ocean Optics) at the fiber exit end. The coupling loss due to scattered light is measured by the fiber-optic probe of another spectrometer (USB4000, Ocean Optics) placed 0.5 mm above the fiber and about 50 mm from the fiber entrance. The fiber transmission property is characterized by the coupling efficiency spectrum (CES), which is measured by a tunable ultrafast oscillator (probe laser) as described previously¹ with the exception that the above aspheric lens is used.

Figures 1(a)–1(e) outline the results of a fiber (~ 1 m) pumped by 210 fs pulses at 200 mW total power. The bandwidth of the SC progressively decreases [Fig. 1(a)] while its power drops from 101 to 43 mW [Fig. 1(d)] over a period of 650 min. Simultaneously, the spectrum of the scattered light becomes increasingly structured [Fig. 1(b)] while its power (i.e., integrated spectral area) progressively increases [Fig. 1(d)]. These changes cannot be compensated by optical realignment. Further irradiation produces no additional effects, indicating the light-matter interaction has attained a steady state. The CES of the fiber evolves into a profile of a longpass filter [Fig. 1(c)], indicating the formation of a waveguide. This waveguide is persistent over time, localized within the first 10 mm from the fiber entrance and erasable by a ~ 3 min candle flame ($T=1620$ K) treatment, just like its counterpart in germanosilicate fibers.¹ These similarities strongly suggest their common origin, which cannot be a photodarkening effect because the PCF is dopant-free. While the bandpass filterlike CES profile of the germanosilicate waveguide can marginally be attributed to a highly defected LPG, the longpass filterlike CES profile of the silica waveguide cannot likely be attributed to this because of the presence of a wide (~ 100 nm) rejection band which may be extended to well below 700 nm (a region outside the tunable range of the probe laser).

Since significant scattering intensity can only be detected at fiber locations where the acrylate coating is present, the scattered light comes from the diffusive cladding-coating interface and should be proportional to the intensity of the light propagated inside the cladding at the probed location. Properly scaled scattering light power is able to compliment the coupling efficiency of the pump laser to produce a sum of $96.0 \pm 1.5\%$ [Fig. 1(e)]. If the Fresnel reflection accounts for

^{a)}Electronic mail: htu@uiuc.edu.

^{b)}Electronic mail: bopp@uiuc.edu.

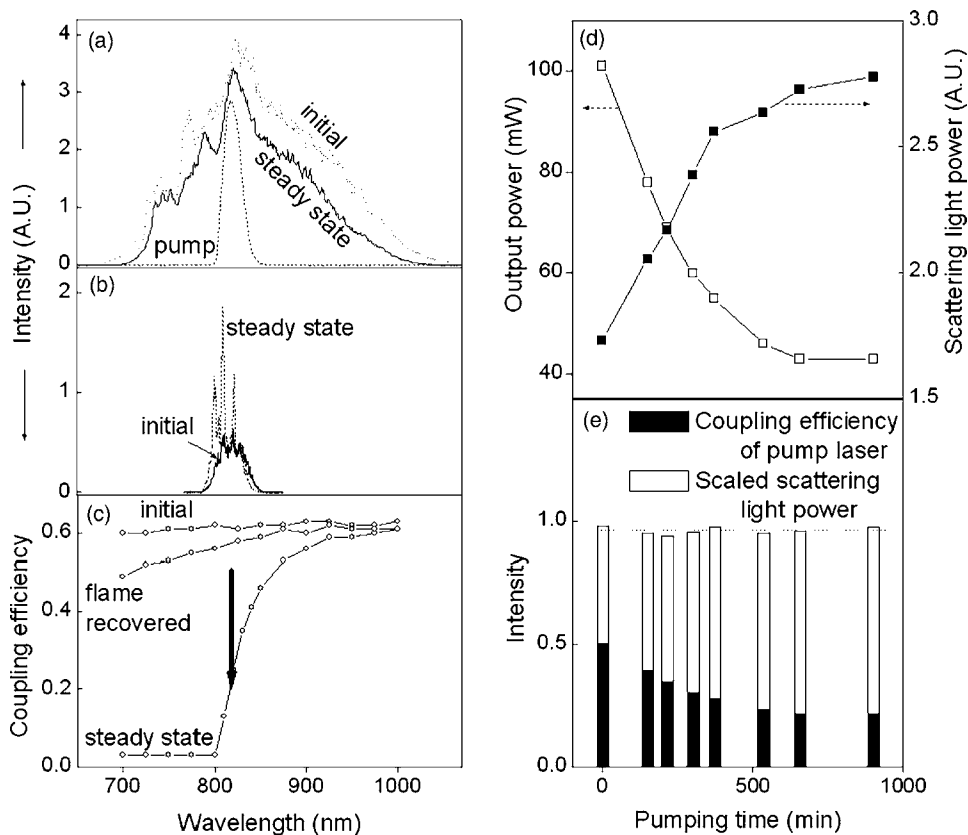


FIG. 1. (a). Initial spectrum and steady state spectrum of the supercontinuum from a LMA-8 fiber under 900 min pumping (818 nm, 210 fs, 200 mW); the spectrum of the pump laser is shown for comparison, (b) initial spectrum (solid line) and steady state spectrum (dotted line) of the scattered light from the fiber, (c) initial, steady state, and flame recovered CES of the fiber; the arrow in the middle of the figure indicates the trace of the coupling efficiency of the pump laser (818 nm) during the pumping process (d) output power and scattering light power from the fiber as a function of pumping time, and (e) complimentary correspondence between the scaled scattering light power and corresponding coupling efficiency of the pump laser as a function of pumping time.

4% coupling loss, the decreasing coupling efficiency can be attributed to waveguide-assisted redistribution (i.e., small angle scattering) of the light from the core (fundamental) mode to the cladding modes, which dissipate along the fiber and do not exit from the fiber end. Thus, the observed transmission loss at the pump wavelength is originating from scattering. Analogous to the photodarkening effect, this photosensitivity can be termed as the photoscattering effect. The increasingly structured spectrum of the scattered light [Fig. 1(b)] is due to the increased waveguide-assisted redistribution of the self-phase-modulation broadened core mode to the cladding modes. The attenuated core mode results in reduced SC bandwidth [Fig. 1(a)]. The same scattering-based redistribution is likely responsible for the transmission loss of <818 nm light [Fig. 1(c)], leading to a nonabsorptive longpass fiber filter which may be useful for wavelength selection in high power applications.

Preliminary results show that the steady state CES of the waveguide depends sensitively on width/chirp, energy, and wavelength of the incident pulses, suggesting the photoinduced waveguide has fine structures of refractive index heterogeneity. The same experiment has been performed at 40 mW pump power for 818 nm 35 fs pulses on another fiber (~ 1 m). The output power drops from 16.0 to 10.4 mW in 310 min and stabilizes thereafter, producing a thermally erasable waveguide with a CES shown in Fig. 2(a). While the waveguide seems to have an uninterestingly broad rejection band, it should be noted that this rejection is invalid for the pump light having high peak pulse intensity. The reason why the transmission property of this waveguide has such an unusual dependence on peak intensity can be understood by monitoring the output power of a fresh fiber (~ 1 m) with increasing input (pump) power after the coupling efficiency

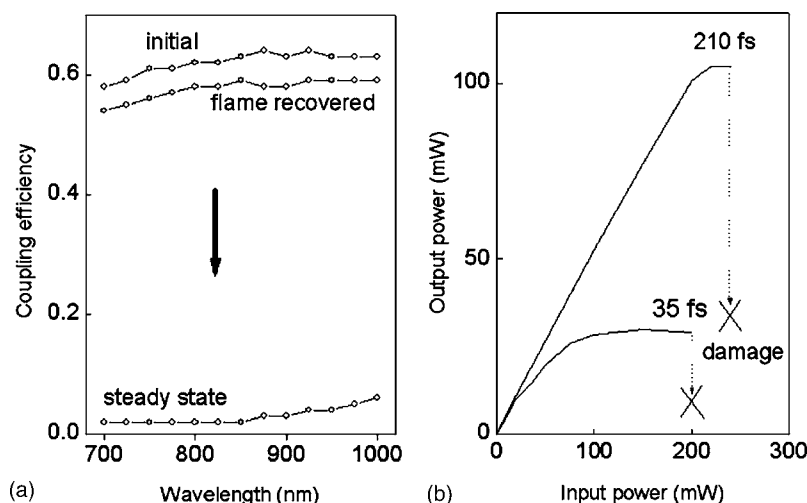


FIG. 2. (a). Initial, steady state, and flame recovered CES of a LMA-8 fiber under 310 min pumping (818 nm, 35 fs, 40 mW); the arrow in the middle of the figure indicates the trace of the coupling efficiency of the pump laser (818 nm) during the pumping process. (b) Output power from a fresh LMA-8 fiber as a function of input power for transform-limited 35 fs incident pulses or positively chirped 210 fs incident pulses at 818 nm.

is maximized at low input power [Fig. 2(b)]. For the 210 fs pulses, the output is roughly proportional to the input until a critical power of 240 ± 20 mW (i.e., damage threshold), where it drops to near zero. For the 35 fs pulses, the output versus input curve is nonlinear at moderate input powers, suggesting the presence of a self-focusing effect. The self-focusing effect at high peak intensity irradiation may overcome the photoscattering effect of the waveguide to enhance transmission. The effect is relatively minor for the 210 fs pulses so that the transmission property of the corresponding waveguide is similar for the pump and probe light [Fig. 1(c)].

The focused spot size of the aspheric lens is $6.5 \mu\text{m}$ (818 nm) so that the damage threshold of the fiber (210 fs) corresponds to a peak intensity of $15 \text{ TW}/\text{cm}^2$. This damage is found to be restricted to within 1 mm from the fiber entrance and cannot be thermally recovered. If the pump power is reduced to 100 mW (210 fs), the CES of the fiber changes a little after 600 min irradiation and the output power and SC spectrum remain relatively stable. Thus, there is a lower threshold of $6\text{--}12 \text{ TW}/\text{cm}^2$ and an upper threshold of $15 \text{ TW}/\text{cm}^2$ which correspond to the formation of the thermally erasable waveguide and the onset of permanent fiber transmission loss, respectively. Such dual-threshold ~ 800 nm photosensitivity has been reported in the microolithography of bulk silica glass,⁵ where the lower and upper thresholds of 7.96 and $9.15 \text{ TW}/\text{cm}^2$ correspond to the formation of thermally erasable low-loss waveguides and thermally inerasable high-loss waveguides,^{5,6} respectively. Similar phenomenon is observed in a germanosilicate fiber,¹ where the lower and upper thresholds of <1 and $2 \text{ TW}/\text{cm}^2$ correspond to the formation of a thermally erasable bandpass filter-type waveguide and the onset of permanent transmission loss, respectively. These coincidences strongly suggest the common origin of the ~ 800 nm photosensitivity associated with the lower threshold. Since it has been attributed to the five-photon absorption of the oxygen deficiency center (I) [ODC(I)] of $\equiv\text{Si}\text{—}\text{Si}\equiv$ in pure silica glass,⁵ it can be similarly attributed to ODC(I)s of $\equiv\text{Ge}\text{—}\text{Si}\equiv$ and $\equiv\text{Ge}\text{—}\text{Ge}\equiv$ in Ge-doped silica glass. The 7.6 eV singlet-singlet transition of $\equiv\text{Si}\text{—}\text{Si}\equiv$ is well documented⁷ while the energy of this transition is nearly identical for $\equiv\text{Si}\text{—}\text{Si}\equiv$, $\equiv\text{Ge}\text{—}\text{Si}\equiv$, and $\equiv\text{Ge}\text{—}\text{Ge}\equiv$.⁸ Thus, the

five-photon absorption of ~ 800 nm (1.55 eV) irradiation excites the transition of these ODC(I)s to induce refractive index modulation responsible for various thermally erasable photonic features. This threshold is defined by experimental sensitivity rather arbitrarily because of the high order power dependence. In contrast, the UV/IR photosensitivity in germanosilicate fiber grating inscription is widely believed to operate on ODC(II) of $\equiv\text{Ge}\cdots\text{Ge}\equiv$ and $\equiv\text{Ge}\cdots\text{Si}\equiv$.⁷

We observe a photosensitivity in supercontinuum-generating pure silica fiber which differs remarkably from that which photodarkens the rare-earth doped fibers or inscribes fiber gratings. In PCF-based SC applications, this photosensitivity is undesirable and may be suppressed by removing the responsible photosensitive species using UV irradiation⁷ or oxygen oxidization.⁹ On the other hand, this photosensitivity can be useful to produce interesting photonic devices such as nonabsorptive bandpass or longpass fiber filters. Improved raw material preparation may enhance this photosensitivity while optimized pumping conditions may engineer the optical properties of the photonic devices. Theoretical studies may follow to decipher the fine structures of the photoinduced waveguides, which, to date, have not been identified by scanning electron microscopy.

This research was supported in part by the National Science Foundation [BES 03-47747, BES 05-19920, and BES 06-19257 (S.A.B.)] and the National Institutes of Health [Roadmap Initiative 1 R21 EB005321 and NIBIB 1 R01 EB005221 (S.A.B.)].

¹H. Tu, D. L. Marks, Y. L. Koh, and S. A. Boppart, *Opt. Lett.* **32**, 2037 (2007).

²J. J. Koponen, M. J. Söderlund, H. J. Hoffman, and S. K. T. Tammela, *Opt. Express* **14**, 11539 (2006).

³D. N. Nikogosyan, *Meas. Sci. Technol.* **18**, 1 (2007).

⁴G. Humbert, W. Wadsworth, S. Leon-Saval, J. Knight, T. Birks, P. S. J. Russell, M. Lederer, D. Kopf, K. Wiesauer, E. Breuer, and D. Stifter, *Opt. Express* **14**, 1596 (2006).

⁵A. Zoubir, C. Rivero, R. Grodsky, K. Richardson, M. Richardson, T. Cardinal, and M. Couzi, *Phys. Rev. B* **73**, 224117 (2006).

⁶A. Zoubir, M. Richardson, L. Canioni, A. Brocas, and L. Sarger, *J. Opt. Soc. Am. B* **22**, 2138 (2005).

⁷L. Skuja, *J. Non-Cryst. Solids* **239**, 16 (1998).

⁸B. B. Stefanov and K. Raghavachari, *Phys. Rev. B* **56**, 5035 (1997).

⁹J. Albert, K. O. Hill, D. C. Johnson, F. Bilodeau, S. J. Mihailov, N. F. Borrelli, and J. Amin, *Opt. Lett.* **24**, 1266 (1999).